Proceedings of the
46th IEEE Conference on Decision and Control
New Orleans, LA, USA, Dec. 12-14, 2007

Motion camouflage in a stochastic setting

K. S. Galloway, E. W. Justh, and P. S. Krishnaprasad

Abstract— **Recent work has formulated 2- and 3-dimensional models and steering control laws for motion camouflage, a stealthy pursuit strategy observed in nature. Here we extend the model to encompass the use of a high-gain pursuit law in the presence of sensor noise as well as in the case when the evader's steering is driven by a stochastic process, demonstrating (in the planar setting) that motion camouflage is still accessible (in the mean) in finite time. We also discuss a family of admissible stochastic evader controls, laying out the groundwork for a future game-theoretic study of optimal evasion strategies.**

I. Introduction

Motion camouflage is a stealthy pursuit strategy which relies on minimizing the perceived relative motion of a pursuer as observed by its prey. The phenomenon of motion camouflage has been biologically documented for visual insects in [16] and in [11] (based on [2]), mathematically characterized (e.g., [4]), and recently analyzed as a deterministic feedback system [9], [13]. Furthermore, a geometrically indistinguishable strategy has been shown to be used by certain echolocating bats intercepting prey insects [3]. The analysis of a feedback law for motion camouflage has been performed in both the planar ([9]) and three-dimensional settings ([13]), using the machinery of curves and moving frames [1]. Close parallels have been shown to exist between motion camouflage (which is rooted in biology), and the Pure Proportional Navigation Guidance (PPNG) law for missile guidance [12], [15]. That motion camouflaged pursuit appears in such diverse contexts has motivated more detailed study of such aspects as sensory feedback delays [14], and the stochastic formulation presented in the present work.

Previous work in [9] and [13] made use of natural Frenet frames [1] to describe the particle trajectories and develop models for the pursuer-evader interaction in a deterministic setting. In this paper we make use of the planar model to investigate the impacts of stochasticity such as sensor noise and evader controls driven by random processes. In the biological setting, we consider possible connections with organisms that appear to use stochastic control processes, such as the "run-and-tumble" movement exhibited in bacterial chemotaxis (see, e.g., [17]). Many species of bacteria use this type of stochastic steering control, which we model as a continuous time, finite state (CTFS) process driven by Poisson counters. (See Section V). Other types of erratic evasion maneuvers utilized by a variety of insects, birds and fish are discussed in [5]. In the vehicular setting, we note possible applications in areas such as aircraft-missile interactions, considering the possibility that some type of stochastic evasive maneuver may in fact prove most effective against an inbound weapon. (We do not consider such issues in the current paper but plan to address the game-theoretic problem in future work.)

We proceed by sketching the planar pursuit-evasion model as well as some of the fundamentals of motion camouflage and the motion camouflage proportional guidance (MCPG) feedback law derived in [9]. In Section III we consider the effects of sensor noise, and in Section IV we address motion camouflage with a stochastically steering evader, stating and proving a proposition that the MCPG law will still ensure attainment of motion camouflage in the mean in finite time. After presenting some specific forms of admissible stochastic controls in Section V and simulation results in Section VI, we conclude by discussing directions for future work.

II. Motion camouflage model

Our starting point is the deterministic planar motion camouflage model described in [9]. A generalization of this deterministic planar model may be found in [13], and the analysis presented here can be generalized to three dimensions using the same techniques. Because here we wish to focus on the novel stochastic elements being introduced into the motion camouflage model, we restrict discussion to the planar setting. Also, to streamline the discussion we assume constant-speed motion and no sensorimotor feedback delays.

A. Trajectory and frame evolution

To keep the discussion as self-contained as possible, we reiterate the basic planar motion camouflage formulation of [9]. Particles moving at constant speed subject to continuous (deterministic) steering controls trace out trajectories which are C^2, i.e., twice continuously differentiable. Without loss of generality, we may assume that the pursuer particle moves at unit speed, and the evader particle moves at speed $\nu > 0$ (i.e., ν corresponds to the ratio of speeds of the pursuer and evader).

This research was supported in part by the Air Force Office of Scientific Research under AFOSR Grant Nos. FA95500410130 and FA9550710446; by the Army Research Office under ARO Grant No. W911NF0610325; by the Army Research Office under ODDR&E MURI01 Program Grant No. DAAD19-01-1-0465 to the Center for Communicating Networked Control Systems (through Boston University); by NIH-NIBIB grant 1 R01 EB004750-01, as part of the NSF/NIH Collaborative Research in Computational Neuroscience Program; and by the Office of Naval Research.

K.S. Galloway and P.S. Krishnaprasad are with the Institute for Systems Research and the Department of Electrical and Computer Engineering at the University of Maryland, College Park, MD 20742, USA. kgallow1@umd.edu, krishna@umd.edu

E.W. Justh is with the Naval Research Laboratory, Washington, DC 20375, USA. eric.justh@nrl.navy.mil

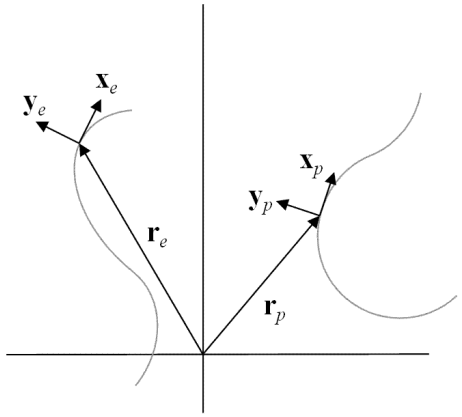

Fig. 1. Illustration of the trajectories and natural Frenet frames for the planar pursuer-evader engagement. (Figure from [9].)

The motion of the pursuer is described by

$$\begin{aligned} \dot{\mathbf{r}}_p &= \mathbf{x}_p, \\ \dot{\mathbf{x}}_p &= \mathbf{y}_p u_p, \\ \dot{\mathbf{y}}_p &= -\mathbf{x}_p u_p, \end{aligned} \tag{1}$$

and the motion of the evader is described by

$$\begin{aligned} \dot{\mathbf{r}}_e &= \nu \mathbf{x}_e, \\ \dot{\mathbf{x}}_e &= \nu \mathbf{y}_e u_e, \\ \dot{\mathbf{y}}_e &= -\nu \mathbf{x}_e u_e, \end{aligned} \tag{2}$$

where the steering control of the evader, u_e, is prescribed, and the steering control of the pursuer, u_p, is given by a feedback law. The orthonormal frame $\{\mathbf{x}_p, \mathbf{y}_p\}$, which is the planar natural Frenet frame for the pursuer particle, evolves with time as the pursuer particle moves along its trajectory (described by $\mathbf{r}_p$). Similarly, $\{\mathbf{x}_e, \mathbf{y}_e\}$ is the planar natural Frenet frame corresponding to the evader particle. (In the planar setting, the natural Frenet frame and the Frenet-Serret frame coincide; however in higher dimensions the distinction is critical [1], [8].)

Here we assume $\nu < 1$, so that the pursuer moves faster than the evader. Figure 1 illustrates (1) and (2). (As noted in [9], the controls u_e and u_p are actually acceleration inputs since they directly drive the angular velocity of the particles. However, the speed for each particle remains constant since the acceleration inputs are constrained to be applied perpendicular to the instantaneous direction of particle motion.)

B. Definition of motion camouflage

In this paper we focus on "motion camouflage with respect to infinity", the strategy in which the pursuer maneuvers in such a way that, from the point of view of the evader, the pursuer always appears at the same bearing. This is described in [9] as

$$\mathbf{r}_p = \mathbf{r}_e + \lambda \mathbf{r}_\infty \tag{3}$$

where $\mathbf{r}_\infty$ is a fixed unit vector and λ is a time-dependent scalar. We define the "baseline vector" as the vector from the evader to the pursuer

$$\mathbf{r} = \mathbf{r}_p - \mathbf{r}_e, \tag{4}$$

and $|\mathbf{r}|$ denotes the baseline length. Restricting ourselves to the non-collision case (i.e. $|\mathbf{r}| \neq 0$), we define $\mathbf{w}$ as the vector component of $\dot{\mathbf{r}}$ which is transverse to $\mathbf{r}$, i.e.

$$\mathbf{w} = \dot{\mathbf{r}} - \left(\frac{\mathbf{r}}{|\mathbf{r}|} \cdot \dot{\mathbf{r}} \right) \frac{\mathbf{r}}{|\mathbf{r}|}. \tag{5}$$

It was demonstrated in [9] that the pursuit-evasion system (1),(2) is in a state of motion camouflage without collision on a given time interval iff $\mathbf{w} = 0$ on that interval.

C. Distance from motion camouflage

The function

$$\Gamma = \frac{\frac{d}{dt}|\mathbf{r}|}{|\frac{d\mathbf{r}}{dt}|} = \left(\frac{\mathbf{r}}{|\mathbf{r}|} \cdot \frac{\dot{\mathbf{r}}}{|\dot{\mathbf{r}}|} \right) \tag{6}$$

describes how far the pursuer-evader system is from a state of motion camouflage [9], [13]. The system is in a state of motion camouflage when $\Gamma = -1$, which corresponds to pure shortening of the baseline vector. (By contrast, $\Gamma = 0$ corresponds to pure rotation of the baseline vector, and $\Gamma = +1$ corresponds to pure lengthening of the baseline vector.) The difference $\Gamma - (-1) > 0$ is a measure of the distance of the pursuer-evader system from a state of motion camouflage.

For (6) to be well defined, we must have $|\mathbf{r}| > 0$ as well as $|\dot{\mathbf{r}}| > 0$. The former requirement is satisfied by assuming that $|\mathbf{r}| \neq 0$ initially, and then analyzing the engagement (for finite time) only until $|\mathbf{r}|$ reaches a value $r_0 > 0$ [9], [13]. The latter condition is ensured by the assumption that $0 < \nu < 1$, since $|\dot{\mathbf{r}}| \geq 1 - \nu$.

D. Feedback law for motion camouflage

We define the notation $\mathbf{q}^\perp$ to represent the vector $\mathbf{q}$ rotated counter-clockwise in the plane by an angle $\pi/2$ [9], [13]. When there is no delay associated with incorporating sensory information, we define our feedback law as

$$u_p = -\mu \left(\frac{\mathbf{r}}{|\mathbf{r}|} \cdot \dot{\mathbf{r}}^\perp \right), \tag{7}$$

where $\mu > 0$ is a gain parameter [9], [13]. However, if there is a delay τ in the incorporation of sensory information, then we substitute $u_p(t - \tau)$ for u_p in equation (1).

Observe that (7) is well defined since, by the discussion in the previous subsection, $|\mathbf{r}| \neq 0$ during the duration of our analysis.

E. Deterministic analysis

The key results for the deterministic motion camouflage feedback system are presented in [9], [13]. These results, particularly the planar result in [9], are the inspiration for the calculations below in Section IV.

III. SENSOR NOISE

One way to introduce stochasticity into the motion camouflage system is through sensor noise [9]. Figure 2, which is taken from [9], illustrates how sensor noise can be incorporated.

In figure 2(a), the dashed dark line is the evader trajectory and the solid dark line is the corresponding pursuer trajectory under control law (7), but with noisy measurements. An $\mathbb{R}^2$-valued independent identically-distributed (iid) discrete-time Gaussian noise process with zero mean and covariance matrix $\text{diag}(\sigma^2, \sigma^2)$, $\sigma = .15|\mathbf{r}|$, is added to the true relative position $\mathbf{r}$ at each measurement instant. Similarly, an $\mathbb{R}^2$-valued iid discrete-time Gaussian noise process with zero mean and covariance matrix $\text{diag}(\tilde{\sigma}^2, \tilde{\sigma}^2)$, $\tilde{\sigma} = .15|\dot{\mathbf{r}}|$, is added to the true relative velocity $\dot{\mathbf{r}}$ at each measurement instant. These two measurement processes are then used by the pursuer to compute (7). The position measurements are superimposed on the true trajectory of the evader, and it can be seen that the absolute measurement error decreases as the relative distance $|\mathbf{r}|$ becomes small. In this simulation, the gain $\mu = 1$, the measurement interval is approximately .5 time units (during which a constant steering control u_p is applied), the pursuer moves at unit speed, and the total simulation time is approximately 1500 time units.

Figure 2(b) shows the corresponding cost function $\Gamma(t)$ given by (6), plotted as a function of time. The difference between $\Gamma(t)$ and -1 measures how far the system deviates from a state of motion camouflage. Part of this deviation is due to the noisy measurements, and part is due to the maneuvering of the evader (because the gain μ is finite).

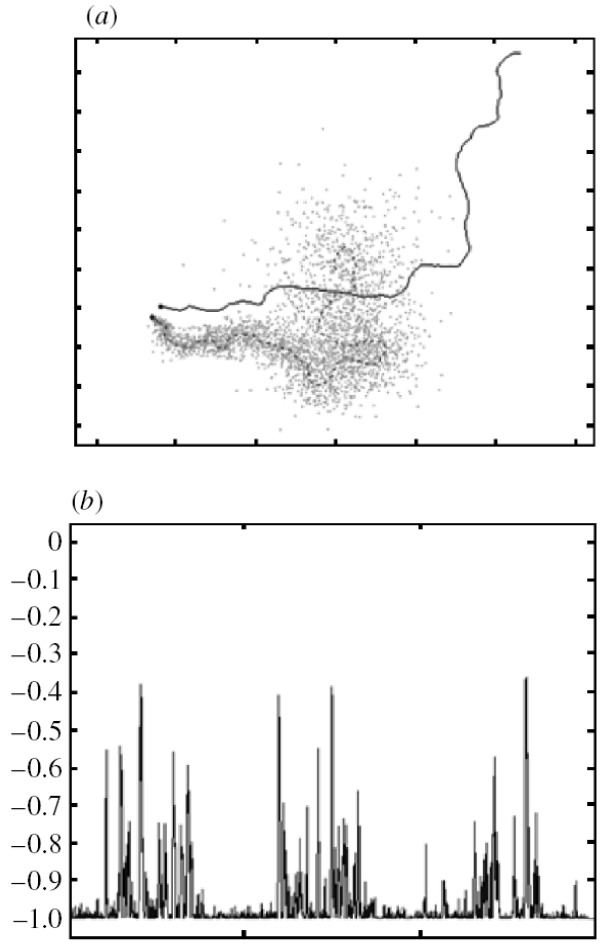

Fig. 2. Pursuit with noisy sensory measurements available to the pursuer: (a) pursuer and evader trajectories, (b) the corresponding distance function Γ as a function of time. (Figure from [9].)

IV. STOCHASTICALLY STEERING EVADER

A. SDE for Γ

Let us now suppose that u_e is not a deterministic function of time, but is instead driven by a stochastic process (in a way we will make precise later). Then $\mathbf{r}$ and $\dot{\mathbf{r}}$ are also stochastic processes, as is Γ given by (6). Analogous to the calculation of $\dot{\Gamma}$ given in [9], we can derive the following SDE (Stochastic Differential Equation) for Γ (see **Remark 5**):

$$\begin{aligned} d\Gamma \;=\; & \frac{|\dot{\mathbf{r}}|}{|\mathbf{r}|}\left[\frac{1}{|\dot{\mathbf{r}}|^2}\left(\frac{\mathbf{r}}{|\mathbf{r}|}\cdot\dot{\mathbf{r}}^{\perp}\right)^2\right]dt \\ & +\frac{1}{|\dot{\mathbf{r}}|}\left[\frac{1}{|\dot{\mathbf{r}}|^2}\left(\frac{\mathbf{r}}{|\mathbf{r}|}\cdot\dot{\mathbf{r}}^{\perp}\right)\right](1-\nu(\mathbf{x}_p\cdot\mathbf{x}_e))u_p dt \\ & +\frac{1}{|\dot{\mathbf{r}}|}\left[\frac{1}{|\dot{\mathbf{r}}|^2}\left(\frac{\mathbf{r}}{|\mathbf{r}|}\cdot\dot{\mathbf{r}}^{\perp}\right)\right](\nu-(\mathbf{x}_p\cdot\mathbf{x}_e))\nu^2 u_e dt, \end{aligned} \tag{8}$$

which is supplemented by the SDE versions of (1) and (2), all of which should be interpreted as stochastic differential equations of the Itô type. Here, as in [9], the notation $\mathbf{q}^{\perp}$ represents the vector $\mathbf{q}$ rotated counter-clockwise in the plane by an angle $\pi/2$. Substituting (7) into (8) gives (c.f., [9])

$$\begin{aligned} d\Gamma \;=\; & -\left[\frac{\mu}{|\dot{\mathbf{r}}|}(1-\nu(\mathbf{x}_p\cdot\mathbf{x}_e))-\frac{|\dot{\mathbf{r}}|}{|\mathbf{r}|}\right]\left[\frac{1}{|\dot{\mathbf{r}}|^2}\left(\frac{\mathbf{r}}{|\mathbf{r}|}\cdot\dot{\mathbf{r}}^{\perp}\right)^2\right]dt \\ & +\frac{1}{|\dot{\mathbf{r}}|}\left[\frac{1}{|\dot{\mathbf{r}}|^2}\left(\frac{\mathbf{r}}{|\mathbf{r}|}\cdot\dot{\mathbf{r}}^{\perp}\right)\right](\nu-(\mathbf{x}_p\cdot\mathbf{x}_e))\nu^2 u_e dt. \end{aligned} \tag{9}$$

Noting that

$$\frac{1}{|\dot{\mathbf{r}}|^2}\left(\frac{\mathbf{r}}{|\mathbf{r}|}\cdot\dot{\mathbf{r}}^{\perp}\right)^2 = 1-\left(\frac{\mathbf{r}}{|\mathbf{r}|}\cdot\frac{\dot{\mathbf{r}}}{|\dot{\mathbf{r}}|}\right)^2 = 1-\Gamma^2, \tag{10}$$

and that $1-\Gamma^2 \geq 0$, we conclude that

$$\begin{aligned} d\Gamma \;\leq\; & -(1-\Gamma^2)\left[\frac{\mu}{|\dot{\mathbf{r}}|}(1-\nu(\mathbf{x}_p\cdot\mathbf{x}_e))-\frac{|\dot{\mathbf{r}}|}{|\mathbf{r}|}\right]dt \\ & +\frac{1}{|\dot{\mathbf{r}}|^2}(\sqrt{1-\Gamma^2})\left|(\nu-(\mathbf{x}_p\cdot\mathbf{x}_e))\nu^2 u_e\right|dt. \end{aligned} \tag{11}$$

Futhermore, as in the deterministic analysis in [9], we have the following inequalities:

$$|\mathbf{x}_p\cdot\mathbf{x}_e| \leq 1, \text{ and } 1-\nu \leq |\dot{\mathbf{r}}| \leq 1+\nu, \tag{12}$$

so that

$$d\Gamma \leq -(1-\Gamma^2)\left[\mu\left(\frac{1-\nu}{1+\nu}\right) - \frac{1+\nu}{|\mathbf{r}|}\right]dt + \frac{\nu^2(1+\nu)}{(1-\nu)^2}\left(\sqrt{1-\Gamma^2}\right)|u_e|dt. \quad (13)$$

For $\mu > 0$, we can define constants $r_0 > 0$ and $c_0 > 0$ such that

$$\mu = \left(\frac{1+\nu}{1-\nu}\right)\left(\frac{1+\nu}{r_0} + c_0\right), \quad (14)$$

and thus

$$\mu \geq \left(\frac{1+\nu}{1-\nu}\right)\left(\frac{1+\nu}{|\mathbf{r}|} + c_0\right), \ \ \forall |\mathbf{r}| \geq r_0. \quad (15)$$

We thus have

$$d\Gamma \leq -(1-\Gamma^2)c_0 dt + \frac{\nu^2(1+\nu)}{(1-\nu)^2}\left(\sqrt{1-\Gamma^2}\right)|u_e|dt, \quad (16)$$

for all $|\mathbf{r}| \geq r_0$.

B. Bounds for $E[\Gamma]$

The next step is to take expected values of both sides of (16), which yields

$$\frac{d}{dt}E[\Gamma] \leq -c_0 E\left[1-\Gamma^2\right] + \frac{\nu^2(1+\nu)}{(1-\nu)^2}E\left[|u_e|\sqrt{1-\Gamma^2}\right], \quad (17)$$

provided $|\mathbf{r}| \geq r_0$. By the Cauchy-Schwartz Inequality,

$$\left|E\left[|u_e|\sqrt{1-\Gamma^2}\right]\right| \leq \sqrt{E\left[u_e^2\right]}\sqrt{E\left[1-\Gamma^2\right]}, \quad (18)$$

from which it follows that

$$\frac{d}{dt}E[\Gamma] \leq -c_0 E\left[1-\Gamma^2\right] + c_1\sqrt{E\left[1-\Gamma^2\right]}, \quad (19)$$

provided $|\mathbf{r}| > r_0$. Here we've assumed that u_e has a bounded second moment (i.e. $E[u_e^2] \leq u_{max}^2$ for some constant $u_{max} > 0$) and we've defined

$$c_1 = \frac{\nu^2(1+\nu)}{(1-\nu)^2}u_{max} > 0. \quad (20)$$

We can now show that, given $0 < \epsilon << 1$, we can choose c_0 (and hence μ) sufficiently large so as to ensure that $dE[\Gamma]/dt \leq 0$ for $E[1-\Gamma^2] > \epsilon$ (provided $|\mathbf{r}| > r_0$). In particular, choose $c_0 > c_1/\sqrt{\epsilon}$. Then (19) becomes

$$\begin{aligned}\frac{d}{dt}E[\Gamma] &\leq -E\left[1-\Gamma^2\right]\left(c_0 - \frac{c_1}{\sqrt{E\left[1-\Gamma^2\right]}}\right)\\ &\leq -E\left[1-\Gamma^2\right]\left(c_0 - \frac{c_1}{\sqrt{\epsilon}}\right)\\ &\leq -E\left[1-\Gamma^2\right]c_2\\ &\leq -c_2\epsilon, \end{aligned} \quad (21)$$

where $c_2 = c_0 - c_1/\sqrt{\epsilon} > 0$, and provided $|\mathbf{r}| > r_0$. Now, (21) can be integrated with respect to time to give

$$E[\Gamma] \leq -c_2\epsilon t + E[\Gamma_0], \quad (22)$$

as long as $E[1-\Gamma^2] > \epsilon$, where $\Gamma_0 = \Gamma(0)$, and provided $|\mathbf{r}| > r_0$.

Because the initial positions $|\mathbf{r}_p(0)|$ and $|\mathbf{r}_e(0)|$ are assumed to be deterministic (even when u_e is stochastic), it follows that $|\mathbf{r}(0)|$ is deterministic. For $r_0 < |\mathbf{r}(0)|$, and using

$$|\mathbf{r}(t)| \geq |\mathbf{r}(0)| - (1+\nu)t, \quad (23)$$

we can conclude that the interval $[0, T)$, where

$$T = \frac{|\mathbf{r}(0)| - r_0}{1+\nu} > 0, \quad (24)$$

is an interval of time over which we can guarantee that $|\mathbf{r}| > r_0$ (regardless of the sample path of u_e).

From the form of (22), it is clear that by choosing c_2 sufficiently large, $E[\Gamma]$ can be driven to an arbitrary negative value at time T, but for the fact that (22) is only valid for $E[1-\Gamma^2] > \epsilon$. Indeed, for any $\eta > 0$ and

$$c_2 > \frac{1+E[\Gamma_0]}{\epsilon T} + \eta, \quad (25)$$

by a contradiction argument, $E[1-\Gamma^2(t_1)] \leq \epsilon$ must hold for some $t_1 \in [0, T)$.

C. Statement of result

Analogously to [9], we define a notion of (finite-time) "accessibility" of the motion camouflage state for the stochastic setting:

Definition 1: Given the system (1) - (2), interpreted as SDEs driven by random processes u_p and u_e having (piecewise) continuous sample paths, we say that "motion camouflage is accessible in the mean in finite time" if for any $\epsilon > 0$ there exists a time t_1 such that $E[1-\Gamma^2(t_1)] \leq \epsilon$.

Proposition 1: Consider the system (1) - (2), with control law (7), and Γ defined by (6), with the following hypotheses:

(A1) $0 < \nu < 1$ (and ν is constant),
(A2) u_e is a stochastic process with piecewise continuous sample paths and bounded first and second moments (i.e. $\exists$ constant $0 < u_{max} < \infty$ such that $\forall t \geq 0$, $E[u_e^2] \leq u_{max}^2$ and $|E[u_e]| \leq u_{max}$),
(A3) u_e is of a form such that the matrix $X = [x_e \quad y_e]$ evolves on $SO(2)$,
(A4) $E[1-\Gamma_0^2] > 0$, where $\Gamma_0 = \Gamma(0)$, and
(A5) $|\mathbf{r}(0)| > 0$.

Then motion camouflage is accessible in the mean in finite time using high-gain feedback (i.e., by choosing $\mu > 0$ sufficiently large.)

Proof: The proof is along the lines of the proof of **Proposition 3.3** in [9] for the deterministic system.

Without loss of generality, we may assume that $E[1-\Gamma_0^2] > \epsilon$.

Choose $r_0 > 0$ such that $r_0 < |\mathbf{r}(0)|$. Choose $c_2 > 0$ sufficiently large so as to satisfy

$$c_2 > \left(\frac{1+\nu}{|\mathbf{r}(0)| - r_0}\right)\left(\frac{1+E[\Gamma_0]}{\epsilon}\right) + \eta, \quad (26)$$

where $\eta > 0$, and choose c_0 as

$$c_0 = c_2 + \frac{1}{\sqrt{\epsilon}} \left(\frac{\nu^2(1+\nu)}{(1-\nu)^2} u_{max} \right). \tag{27}$$

Then defining μ according to (14) ensures that $E[1 - \Gamma^2(t_1)] \leq \epsilon$ for some $t_1 \in [0, T)$, where T is given by (24). □

Remark 1: **Definition 1** above does not distinguish between motion camouflage with decreasing baseline distance (i.e., $\Gamma = -1$) and motion camouflage with increasing baseline distance (i.e., $\Gamma = +1$). By contrast, the definition of finite-time accessibility of motion camouflage given in [9] deals only with decreasing baseline distance.

Remark 2: Assumption (A3) equates to ensuring that the associated vector equation evolves on a circle. This is discussed in the following section.

V. Admissible stochastic controls

In considering the possible families of stochastic processes that could serve as controls for the evader, we can only select such controls that will cause the "rotation matrix" $X = [x_e \quad y_e]$ to evolve on $SO(2)$, the special orthogonal group in two dimensions. For a stochastic u_e, (2) provides the stochastic differential equation

$$dX_t = X_t \hat{A} u_e dt, \tag{28}$$

where $\hat{A}$ is the skew-symmetric matrix defined by

$$\hat{A} = \begin{pmatrix} 0 & -\nu \\ \nu & 0 \end{pmatrix}. \tag{29}$$

Let $x_0 \in \mathbb{R}^2$ and define x_t by $x_t^T = x_0^T X_t$. Then we have

$$dx_t^T = x_t^T \hat{A} u_e dt \Longrightarrow dx_t = \hat{A}^T x_t u_e dt. \tag{30}$$

It can be shown (see, e.g., [10]) that X_t evolves on $SO(2)$ if and only if (30) evolves on a circle.

Proposition 2: Let the stochastic evader control u_e be defined as follows:

$$\begin{aligned} dz &= \alpha(z,t)dt + \beta(z,t)dW, \;\; z(0) = z_0, \\ u_e &= z, \end{aligned} \tag{31}$$

where z is a scalar stochastic process, $W(\cdot)$ is standard Brownian motion, $\alpha : \mathbb{R} \times [0, \infty) \to \mathbb{R}$ and $\beta : \mathbb{R} \times [0, \infty) \to \mathbb{R}$ (and suitable technical hypotheses are met). Then (28) evolves on $SO(2)$.

Proof: Grouping (30) and (31) and dropping the time subscripts for simplicity, we have

$$d \begin{bmatrix} x \\ z \end{bmatrix} = \begin{bmatrix} \hat{A}^T x z \\ \alpha(z) \end{bmatrix} dt + \begin{bmatrix} 0 \\ \beta(z) \end{bmatrix} dW. \tag{32}$$

Let

$$y = \begin{bmatrix} x \\ z \end{bmatrix}, \;\; f(y) = \begin{bmatrix} \hat{A}^T x z \\ \alpha(z) \end{bmatrix}, \text{ and } g(y) = \begin{bmatrix} 0 \\ \beta(z) \end{bmatrix}. \tag{33}$$

Then (32) becomes

$$dy = f(y)dt + g(y)dW. \tag{34}$$

Letting $\psi(y) = x^T x$ and using Itô's rule for differentiating, we have

$$\begin{aligned} d(x^T x) &= d\psi(y) \\ &= \left[\frac{\partial \psi}{\partial t} + \frac{\partial \psi}{\partial y} \cdot f + \frac{1}{2} \text{tr} \left(\frac{\partial^2 \psi}{\partial y \partial y^T} g g^T \right) \right] dt \\ &\quad + \left(\frac{\partial \psi}{\partial y} \cdot g \right) dW \\ &= \begin{bmatrix} 2x \\ 0 \end{bmatrix} \cdot \begin{bmatrix} \hat{A}^T x z \\ \alpha(z) \end{bmatrix} dt \\ &\quad + \frac{1}{2} \text{tr} \left(\begin{bmatrix} 2 & 0 \\ 0 & 0 \end{bmatrix} \begin{bmatrix} 0 & 0 \\ 0 & \beta^2(z) \end{bmatrix} \right) dt \\ &\quad + \begin{bmatrix} 2x \\ 0 \end{bmatrix} \cdot \begin{bmatrix} 0 \\ \beta(z) \end{bmatrix} dW \\ &= 2x^T \hat{A}^T x z dt \\ &= 0, \end{aligned} \tag{35}$$

where the last step follows from the skew-symmetry of $\hat{A}^T$. Equation (35) implies that $x^T x = x_0^T x_0$ for all times $t \geq 0$ (i.e., (30) evolves on a circle), and therefore (28) evolves on $SO(2)$. □

Remark 3: A similar result can be proved for counter-driven stochastic controls of the form

$$\begin{aligned} dz &= \alpha(z,t)dt + \sum_{i=1}^{m} \beta_i(z,t) dN_i, \;\; z(0) = z_0, \\ u_e &= z, \end{aligned} \tag{36}$$

where N_i, $i = 1, 2, ..., m$ are Poisson counters with rates λ_i. (Follow the previous proof and use Itô's rule for jump processes.) □

We note the following specific possibilities for stochastic controls:

(a) Brownian motion. Letting $\alpha(z,t) = 0$ and $\beta(z,t) = 1$ in (31) results in

$$dz = dW, \;\; z(0) = z_0, \;\; u_e = z, \tag{37}$$

i.e., $u_e(\cdot) = W(\cdot)$. In this case, the steering control would be governed by sample paths of a Brownian motion process. However, this control does not satisfy assumption (A2) of **Proposition 1** and is therefore not admissible.

(b) Brownian motion with viscous damping. Let $\alpha(z,t) = -\delta z$ and $\beta(z,t) = \sigma$ for constants $\delta > 0$ and $\sigma \in \mathbb{R}$. Then (31) becomes

$$dz = -\delta z dt + \sigma dW, \;\; z(0) = z_0, \;\; u_e = z, \tag{38}$$

which is better known as the *Langevin equation*. This control satisfies both (A2) and (A3) and is therefore admissible.

(c) "Run-and-tumble" (bacterial chemotaxis). In (36) let $\alpha(z,t) = 0$ and define the Poisson counter rates and coefficients as follows:

$$\begin{aligned}\beta_1(z,t) &= \frac{1}{2}z(z-1),\\ \beta_2(z,t) &= -\frac{1}{2}z(z+1),\\ \beta_3(z,t) &= (z^2-1),\\ \beta_4(z,t) &= -(z^2-1),\\ \lambda_1 &= \lambda_2 = \lambda_H,\\ \lambda_3 &= \lambda_4 = \lambda_L. \end{aligned} \tag{39}$$

Then (36) becomes

$$\begin{aligned} dz &= \frac{1}{2}z(z-1)dN_1 - \frac{1}{2}z(z+1)dN_2\\ &\quad +(z^2-1)dN_3 - (z^2-1)dN_4, \;\; z(0)=z_0,\\ u_e &= z, \end{aligned} \tag{40}$$

and u_e is a continuous time, finite state (CTFS) process taking values in the set $\{-1,0,1\}$. Hence u_e satisfies (A2) and (A3) and is admissible as a stochastic control for the evader. We can approximate bacterial chemotaxis, the "run-and-tumble" control used by certain types of bacteria to move towards food sources, by choosing $\lambda_H >> \lambda_L$. Under this open-loop control, the evader will move primarily in straight paths ($u_e = 0$), making occasional random short-duration turns whenever Poisson counter N_3 or N_4 fires. This could also be implemented as a closed-loop control by feeding state information (such as range to the pursuer) back to the counter rates λ_H and λ_L.

Remark 4: Note that the control $u_e dt = dw$ (i.e., $u_e \approx$ "white noise") is not a permissible control for the evader, since a calculation similar to (35) yields

$$d(x^T x) = x^T \hat{A}\hat{A}^T x dt = \nu^2 x^T \begin{bmatrix} 0 & 1 \\ 1 & 0 \end{bmatrix} x dt, \tag{41}$$

which is not necessarily zero, and therefore $X = [x_e \;\; y_e]$ will not evolve on $SO(2)$. □

Remark 5: Under assumptions (A2) and (A3) referred to above (we are specifically interested in u_e processes such as (38) and (40)), it follows that for each path of u_e, the random differential equations (1),(2) with control (7), have well-defined local pathwise solutions away from collisional states $\mathbf{r}_p = \mathbf{r}_e$. Applying Itô's rule to the ensemble process (1),(2),(7) gives us (8).

VI. Simulation Results

The following simulation results demonstrate the effectiveness of the pursuit law (7) against an evader using a "run-and-tumble" steering control as described in the previous section, confirming the analytical results presented in Section IV. Each simulation is based on the same parameters but differs by the ratio of the Poisson counter rates λ_L and λ_H. (Note also that each simulation was run for approximately 250 time units in steps of .1 time units, and the ratio of

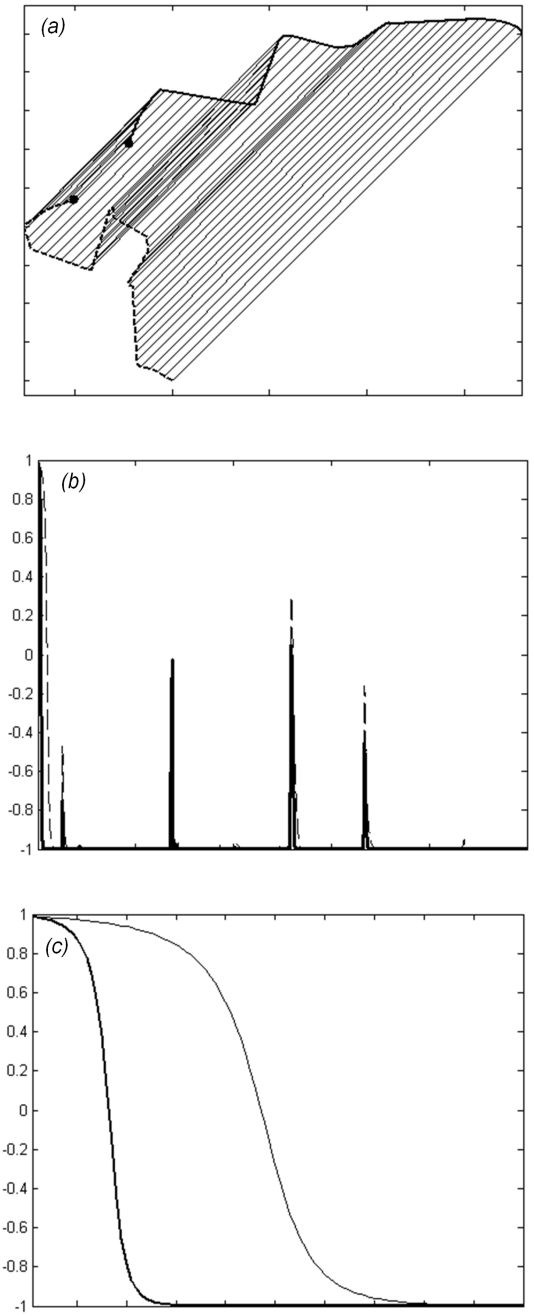

Fig. 3. (a) Evader trajectory with counter-driven "run-and-tumble" steering control (dashed dark line), and the corresponding pursuer trajectory (solid dark line) evolving according to (1) with control given by (7). In this case, $\lambda_H = 40\lambda_L$. (b) The corresponding cost function $\Gamma(t)$ given by (6), plotted as a function of time. The lighter dashed lines correspond to a small value of μ while the darker solid lines correspond to a value of μ which is three times larger. (c) The transient behavior of $\Gamma(t)$ as represented by an initial time interval 1/25th the duration of that displayed in (b). The darker line corresponds to the higher value of μ.

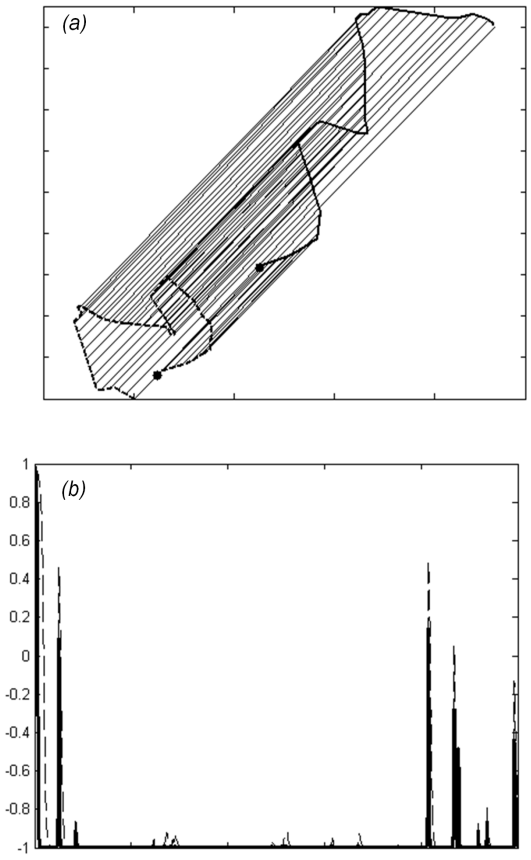

Fig. 4. (a) Pursuer and evader trajectories for a "run-and-tumble" evader steering control with $\lambda_H = 20\lambda_L$. (b) The corresponding cost function $\Gamma(t)$ given by (6), plotted as a function of time. (Note that the transient behavior of $\Gamma(t)$ in this simulation was identical to that from figure 3 and was therefore omitted.)

evader's speed to pursuer's speed was fixed at $\nu = .9$.) Figure 3(a) shows the pursuer and evader trajectories for a simulation in which the ratio between the counter rates is very large ($\lambda_H = 40\lambda_L$) and therefore the evader makes fewer maneuvers. (The lighter lines connecting the pursuer and evader at regular time intervals indicate the evolution of the baseline vector **r**. If the system (1),(2) is in a state of motion camouflage, these lines will be parallel.) Figures 3(b) and 3(c) show the complete and transient behavior, respectively, of the cost function $\Gamma(t)$ given by (6). (Each graph shows the results for both a smaller pursuit feedback gain μ as well as the results for a gain three times larger.) Note that the cost function is driven to the desired value of -1 (indicating attainment of motion camouflage) with intermittent spikes corresponding to momentary deviations from the motion camouflage state. These spikes correspond to time instances when the evader executes an abrupt turn.

Figures 4 and 5 show results for increasingly larger values of λ_L with a fixed λ_H (i.e. higher probability of evader maneuvering.) As demonstrated in figure 5(a), increased evader maneuvering induces more frequent steering requirements for the pursuer, indicating that, while such an evasive

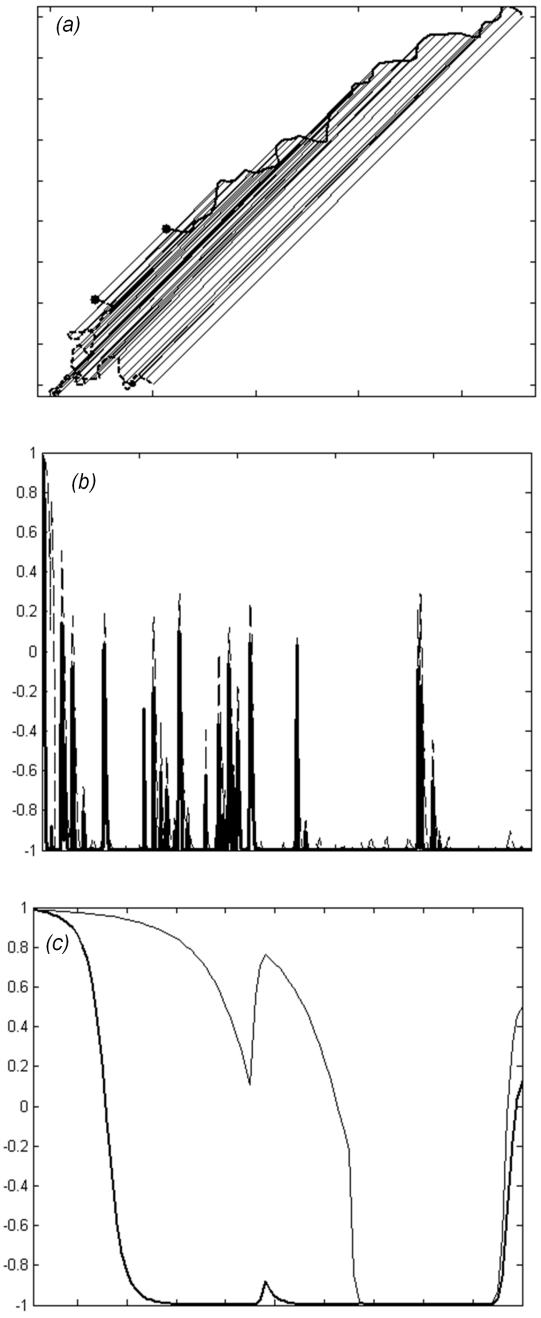

Fig. 5. (a) Pursuer and evader trajectories for a "run-and-tumble" evader steering control with $\lambda_H = 6.67\lambda_L$. (b) The corresponding cost function $\Gamma(t)$ given by (6). (c) The initial behavior of $\Gamma(t)$ over 1/25th of the simulation.

control may not prevent capture, it may introduce a high steering/attention cost on the pursuer. Note from figure 5(b) that the highly erratic evader steering control produced by large values of λ_L (i.e. smaller ratios of λ_H to λ_L) results in frequent deviations from motion camouflage. Figure 5(c) displays the initial transient behavior of $\Gamma(t)$. In the case of the larger value of μ, the initial behavior of $\Gamma(t)$ is similar to that of figure 3(c) since the pursuer is able to maneuver into a motion camouflage state prior to the evader's first course change. For the smaller value of μ, the first evader maneuver occurs while $\Gamma(t)$ is still much larger than -1, thereby delaying convergence to the motion camouflage state.

VII. Directions for future work

In both the deterministic analysis of motion camouflage in [9], [13] and in the stochastic analysis presented here, the speeds of both the pursuer and evader have been constrained to be deterministic (though possibly varying in [13]), with bounds to ensure that the evader's speed is strictly less than that of the pursuer. Our investigation of the effects of stochastic evader behavior could therefore be extended to permit stochastic variation of speed, prompting several interesting questions. While the current work has demonstrated that a pursuer can always attain a state of motion camouflage if the evader's speed is deterministic and slower than the pursuer's, it could also be asked whether the result will still hold if the evader's speed is slower only on average or if the evader's speed is governed by a stochastic process with a particular mean function. Additionally, in our discussion of motion camouflage in both the deterministic and stochastic settings, we have only permitted the evader to use an open-loop strategy rather than a feedback strategy (whereas the pursuer uses a feedback strategy). In the language of biologists, such engagements would more properly be called "pursuer-pursuee" engagements, rather than pursuer-evader engagements. The problem could be reformulated in the context of a differential game (as described in [6], [7]) in which the pursuer would adopt a strategy to intercept the evader (or maximize stealth), and the evader would adopt a strategy to elude the pursuer (or maximize pursuer "visibility"). These types of feedback strategies could be implemented in the stochastic setting by using feedback to regulate parameters of the stochastic process (e.g. varying the rates of the evader's Poisson counters as a function of pursuer range.) In the context of this type of differential game, a family of varying pay-off functions and control constraints could be used to explore possible connections to behaviors observed in biology. The run-and-tumble motion of bacteria and the skittish darting of fish may be consistent with such a formulation.

References

[1] R.L. Bishop, "There is more than one way to frame a curve," *The American Mathematical Monthly*, Vol. 82, No. 3, pp. 246-251, 1975.

[2] T.S. Collett and M.F. Land, "Visual control of flight behaviour in the hoverfly, *Syritta pipiens*," *J. comp. Physiol.*, vol. 99, pp. 1-66, 1975.

[3] K. Ghose, T. Horiuchi, P.S. Krishnaprasad and C. Moss, "Echolocating bats use a nearly time-optimal strategy to intercept prey," *PLoS Biology*, 4(5):865-873, e108, 2006.

[4] P. Glendinning, "The mathematics of motion camouflage," *Proc. Roy. Soc. Lond. B*, Vol. 271, No. 1538, pp. 477-481, 2004.

[5] D. A. Humphries and P. M. Driver, "Erratic Display as a Device against Predators," *Science*, Vol. 156, No. 3783, pp. 1767 - 1768, 1967.

[6] R. Isaacs, *Differential Games*, New York: John Wiley and Sons, 1965.

[7] T. Başar and G. Jan Olsder, *Dynamic Noncooperative Game Theory*, 2nd ed., San Diego: Academic Press, 1995.

[8] E.W. Justh and P.S. Krishnaprasad, "Natural frames and interacting particles in three dimensions," *Proc. 44th IEEE Conf. Decision and Control*, 2841-2846, 2005 (see also arXiv:math.OC/0503390v1).

[9] E.W. Justh and P.S. Krishnaprasad, "Steering laws for motion camouflage," *Proc. R. Soc. A*, Vol. 462, pp.3629-3643, 2006 (see also arXiv:math.OC/0508023).

[10] R.W. Brockett, "Lie algebras and Lie groups in control theory," in D. Q. Mayne and R. W. Brockett, Eds., *Geometric Methods in System Theory*, Dordrecht, Holland: Reidel, pp. 43-82, 1973.

[11] A.K. Mizutani, J.S. Chahl, and M.V. Srinivasan, "Motion camouflage in dragonflies," *Nature*, Vol. 423, p. 604, 2003.

[12] J.H. Oh and I.J. Ha, "Capturability of the 3-dimensional pure PNG law," *IEEE Trans. Aerospace. Electr. Syst.*, Vol. 35, No. 2, pp. 491-503, 1999.

[13] P.V. Reddy, E.W. Justh and P.S. Krishnaprasad, "Motion camouflage in three dimensions," *Proc. 45th IEEE Conf. Decision and Control*, pp. 3327-3332, 2006 (see also arXiv:math.OC/0603176).

[14] P.V. Reddy, E.W. Justh and P.S. Krishnaprasad, "Motion camouflage with sensorimotor delay," to appear, *Proc. 46th IEEE Conf. Decision and Control*, 2007.

[15] N.A. Shneydor, *Missile Guidance and Pursuit*, Horwood, Chichester, 1998.

[16] M.V. Srinivasan and M. Davey, "Strategies for active camouflage of motion," *Proc. Roy. Soc. Lond. B*, Vol. 259, No. 1354, pp. 19-25, 1995.

[17] H.C. Berg and D.A. Brown, "Chemotaxis in *Escherichia coli* analyzed by three-dimensional tracking," *Nature*, Vol. 239, pp. 500-504, 1972.